Optimal 6 Degrees-of-Freedom Station-Keeping of a Satellite in a Cislunar Halo Orbit via Lie Algebra based Convex Model Predictive Control

Minyoung Ra and Joseph Le
Purdue University, West Lafayette, IN, 47906

I. Introduction

Over the past few decades, there have been numerous spacecraft that make use of a special feature of three-body gravitational points known as Lagrange points. The points are dynamical equilibrium points for a small mass object experiencing gravitational forces from two more massive objects. At these points, the gravitation forces of the two larger bodies, and the centrifugal force caused by the objects orbital motion, cancel each other out. This allows a spacecraft placed at one of these points to remain stationary relative to the rotating frame of two primary bodies, making Lagrange points advantageous for certain spacecraft. There are five Lagrange points, two of which are stable, while the other three are an unstable equilibrium. For this project, the unstable L_2 point is considered. This point lies directly away from the Earth and the Moon, making it an ideal position for a space telescope like the JWST and a space station like Lunar Gateway. The Artemis project has conducted test flights on halo orbits around Earth-Moon L_2 point, as shown in Fig. 1. Future projects of Artemis include establishment of Lunar Gateway, a space station orbiting on a southern halo orbit around Earth-Moon L_2 point. This project will study the optimal control for station keeping of a spacecraft near the L_2 point in order to find insight that may be generalized to controlling around other Lagrange points. In a typical space mission, the spacecraft state to be controlled is both position and attitude, and it is referred to as relative 6 degrees-of-freedom (6DOF). In non-linear dynamical environments such as the Cislunar space, both translational and rotational motions are often volatile, leading the uncontrolled object deviate from a reference behavior over time. For a typical multi-spacecraft mission, proximity operation and formation flight of two or more spacecrafts are included. Control of such operations requires coupling between relative attitude and position taken into consideration.

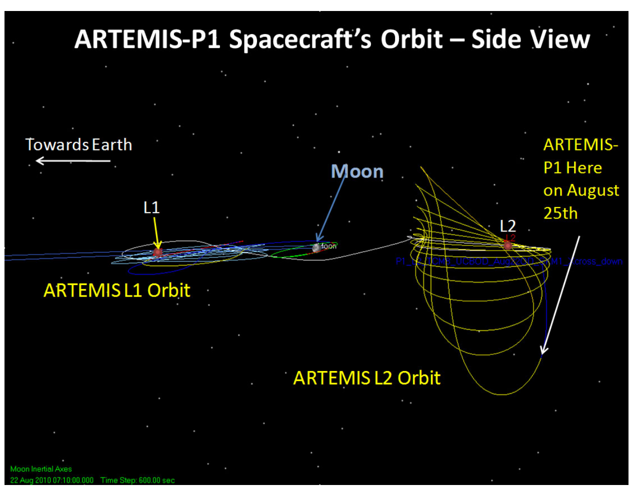

Fig. 1 Artemis-P1 Trajectory in Cislunar Space

Understanding the dynamics of the three-body model is necessary to solving such a problem. The nature of the model in question allows some simplifying assumptions to be made. As already mentioned, the spacecraft is assumed to have a much smaller mass, allowing the three-body problem to be restricted. Additionally, it can be assumed that the larger bodies move in circular orbits. This provides the setup for what is called the circular restricted three-body problem (CR3BP).

II. Existing Work

The multi-body problem formulation and partial solutions for few restricted gravitational model configuration have been suggested over the last century. To better formulate the problem and ease the approach, understanding of the model of interest and reviewing previous works were necessary.

After Howell [1] introduced the general guidance to describing the motion of halo orbits using numerical methods, Howell and Pernicka [2] further investigated station-keeping problem of near-halo orbits, given that the objective of a spacecraft to stay on the nominal paths. As discussed in [1], a nominal path could be numerically solved for any discrete time span and appropriate initial states. Using the nominal path state information, the positional and velocity error can be calculated from the measured values. Many engineers and scientists, including Oguri et al.[3], have analyzed the optimal control problem with Gaussian Distributed perturbation on measured values. Methods to minimize perturbations of the system were also researched.

III. Problem Formulation

A. Model Dynamics

1. Translational Motion

The motion of the spacecraft is described by the gravitational forces of the Earth and Moon. It can be assumed that the motion of the Earth and the Moon due to the gravitation force of the spacecraft is negligible due to the spacecrafts relatively low mass. The primary reference frame that will be used is the synodic frame where $\hat{x}$ is the unit vector pointing from the Earth to the Moon, $\hat{y}$ completes the orthogonal set with $\hat{x}$ and $\hat{z}$, and $\hat{z}$ is the unit vector perpendicular to ecliptic. The secondary reference frame is an the inertial frame ($\hat{X}$,$\hat{Y}$,$\hat{Z}$) which is fixed in the Earth.

For such a problem the state vector can be formulated from the position and velocity of the spacecraft in each direction (in the synodic frame):

$$\boldsymbol{x} = \begin{bmatrix} x & y & z & \dot{x} & \dot{y} & \dot{z} \end{bmatrix}^T$$

These position and velocity values are normalized to the Earth-Moon distance. Additionally, the angular velocity of the Earth and Moon with respect to the center of mass is normalized. These two factors simplify the equations and denormalizing the solution is simple. To further aid in calculations, three parameters are defined: a mass ratio μ which is the ratio of the Moon's mass to the mass of the model, an Earth-distance parameter d which is the normalized distance between the spacecraft and the Earth, and a Moon-distance parameter r which is the normalized distance between the spacecraft and the Moon.

$$\mu = \frac{m_2}{m_1 + m_2} \tag{1}$$

$$\begin{aligned} d &= \sqrt{(x+\mu)^2 + y^2 + z^2} \\ r &= \sqrt{(x-(1-\mu))^2 + y^2 + z^2} \end{aligned} \tag{2}$$

It is also useful to introduce a control vector $\mathbf{u} = \begin{bmatrix} u_x & u_y & u_z \end{bmatrix}^T$, which represents the acceleration due to thrust of the spacecraft in each axis. The CR3BP equations of motion in the synodic frame can be written as follows:

$$\begin{aligned} \ddot{x} &= 2\dot{y} + x - \frac{(1-\mu)(x+\mu)}{d^3} - \frac{\mu(x-1+\mu)}{r^3} + u_x \\ \ddot{y} &= -2\dot{x} + y - \frac{(1-\mu)y}{d^3} - \frac{\mu y}{r^3} + u_y \\ \ddot{z} &= -\frac{(1-\mu)z}{d^3} + \frac{\mu z}{r^3} + u_z \end{aligned} \tag{3}$$

2. Rotational Motion

Suppose the angular momentum about the center of body in synodic frame is $\boldsymbol{H}_S$, the rate of it using the transport theorem is expressed as:

$$ {}^{S}\dot{\boldsymbol{H}}_{S} = {}^{\mathcal{B}}\dot{\boldsymbol{H}}_{S} + {}^{B}\boldsymbol{\omega}^{S}\boldsymbol{H}_{S} = \boldsymbol{L}_{c\,S} \tag{4} $$

Assuming torque-free motion, $\boldsymbol{L}_{c\,S} = 0$, and ${}^{\mathcal{B}}\dot{\boldsymbol{H}}_{S} = \boldsymbol{I}_c \cdot {}^{B}\dot{\boldsymbol{\omega}}^{S}$,

$$ \boldsymbol{I}_c \cdot {}^{B}\dot{\boldsymbol{\omega}}^{S} = -{}^{B}\boldsymbol{\omega}^{S} \times \boldsymbol{I}_c \cdot {}^{B}\boldsymbol{\omega}^{S} \tag{5} $$

The dynamics of the spacecraft's rotational motion in CR3BP is then:

$$ \dot{\omega} = \begin{cases} -K_1\left(\omega_2\omega_3\right) + L_1 \\ -K_2\left(\omega_1\omega_3\right) + L_2 \\ -K_3\left(\omega_1\omega_2\right) + L_3 \end{cases} \tag{6} $$

where L_i are the applied control inputs and K_i are as follows:

$$ \begin{aligned} K_1 &= \frac{I_3 - I_2}{I_1} \\ K_2 &= \frac{I_1 - I_3}{I_2} \\ K_3 &= \frac{I_2 - I_1}{I_3} \end{aligned} \tag{7} $$

B. Reference State History

The Lagrange points themselves occur at locations where the gradient of the model pseudopotential is zero. This pseudopotential is defined as the sum of the gravitation potential plus the apparent potential that results from the centripetal force of the rotating reference frame. The equation is as follows:

$$ V(x, y, z) = -\frac{1}{2}(x^2 + y^2) - \frac{1-\mu}{d} - \frac{\mu}{r} \tag{8} $$

The location of the Lagrange points can be calculated as the solutions to quintic equations. Using Newton's method, the location of L_2 in Cislunar space is obtained as below:

$$ L_2 = \begin{bmatrix} 1.1557 & 0 & 0 \end{bmatrix} \tag{9} $$

By linearizing Eq. 3 the initial estimation on creating periodic orbit was performed. And the initial states that create periodic orbit in the non-linear dynamics were acquired through differential correction methods using Newton's method. With step-size of $\Delta s = 0.0001$, a family of Earth-Moon L_2 southern halo orbits were calculated and is shown in Fig. 2.

In this project, the objective is to maintain a reference attitude while staying on a reference closed-orbit, where the reference is one of the projected Artemis program components, Lunar Gateway. Although the projected orbit of the Gateway is in fact a near-rectilinear halo orbit (NRHO) due to natural perturbations and instability (Fig. 3), this project models the perturbations and instability separately as Gaussian noise to have the reference orbit as a closed halo orbit.

With a closed reference orbit assumption and fixed-attitude assumption, a simulation with no control was run and the result is shown in Fig. 4. As the figure shows, the attitude of the spacecraft is not fixed, and one of the major goals of this project is to fixate the attitude to a desired reference attitude while maintaining nominal orbital path.

C. Lie Algebra

Lie group is a class of groups with the smooth property that indicates the continuity in real space. SE(3) is a special Lie group, which could be characterized by the following homogeneous coordinate form:

$$ \mathrm{SE}(3) = \left\{ \mathcal{H} = \begin{bmatrix} \boldsymbol{P} & \boldsymbol{b} \\ \boldsymbol{0}^T & 1 \end{bmatrix} \in \mathbb{R}^{4\times4} \middle| \boldsymbol{P} \in \mathrm{SO}(3), \quad \boldsymbol{b} \in \mathbb{R}^3, \quad \boldsymbol{0} = \begin{bmatrix} 0 & 0 & 0 \end{bmatrix}^T \right\} \tag{10} $$

where SO(3) is defined as:

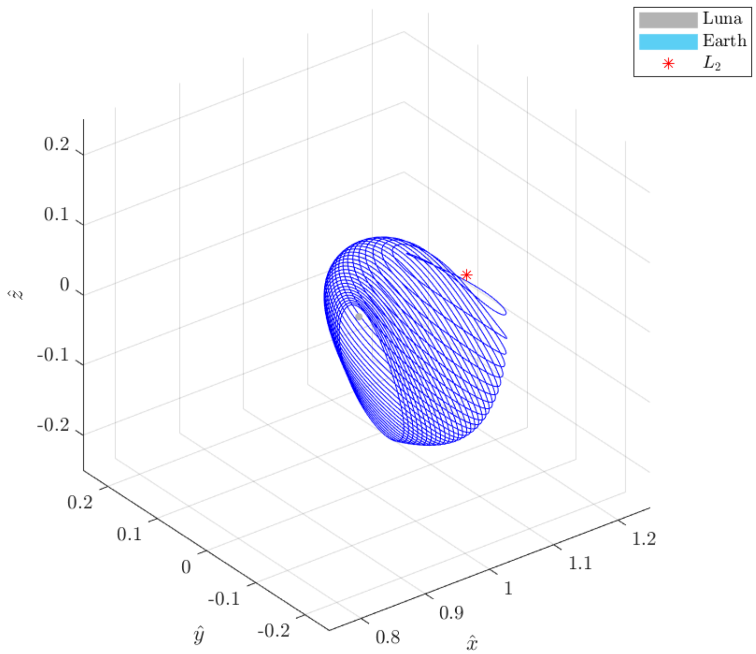

Fig. 2 Earth-Moon L_2 Southern Halo Orbit Family

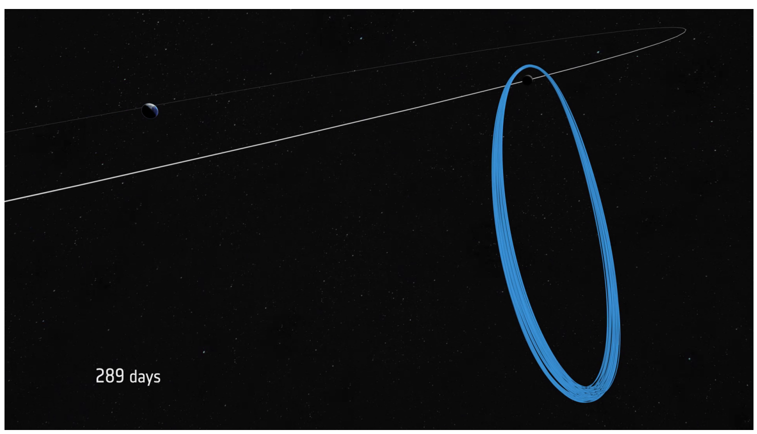

Fig. 3 Projected Artemis Lunar Gateway Orbit (credit: ESA)

$$\mathrm{SO}(3) = \left\{ \boldsymbol{P} \in R^{3\times 3} \mid \boldsymbol{P}^T \boldsymbol{P} = \boldsymbol{I}_3, \quad \det(\boldsymbol{P}) = 1 \right\} \tag{11}$$

We can see that SE(3) does play a beneficial role in convex optimization as it transforms non-linear 6DOF transformation into linear 6DOF transformation with one matrix, i.e., $f(\boldsymbol{a}) = \boldsymbol{P}\boldsymbol{a} + \boldsymbol{b} \rightarrow g(\tilde{\boldsymbol{a}}) = \mathcal{H}\tilde{\boldsymbol{a}}, \tilde{\boldsymbol{a}} = \begin{bmatrix} \boldsymbol{a} & 1 \end{bmatrix}^T$. SE(3) is therefore well referred to as a homongenous affine 6DOF transformation matrix. To describe the local property of the Lie group, the Lie algebra is introduced; set $\mathfrak{so}(3)$, associated with Lie group SO(3), is expressed as:

$$\mathfrak{so}(3) = \left\{ A = \boldsymbol{o}^{\times} = \begin{bmatrix} 0 & -o_3 & o_2 \\ o_3 & 0 & -o_1 \\ -o_2 & o_1 & 0 \end{bmatrix} \in \mathbb{R}^{3\times 3} \mid \boldsymbol{o} \in \mathbb{R}^3 \right\} \tag{12}$$

where any $(\cdot)^{\times}$ represent the cross product operator matrix. $\mathfrak{so}(3)$ is also a linear transformation, therefore is an affine function as well. Set $\mathfrak{se}(3)$ is associated with SE(3), and is defined as:

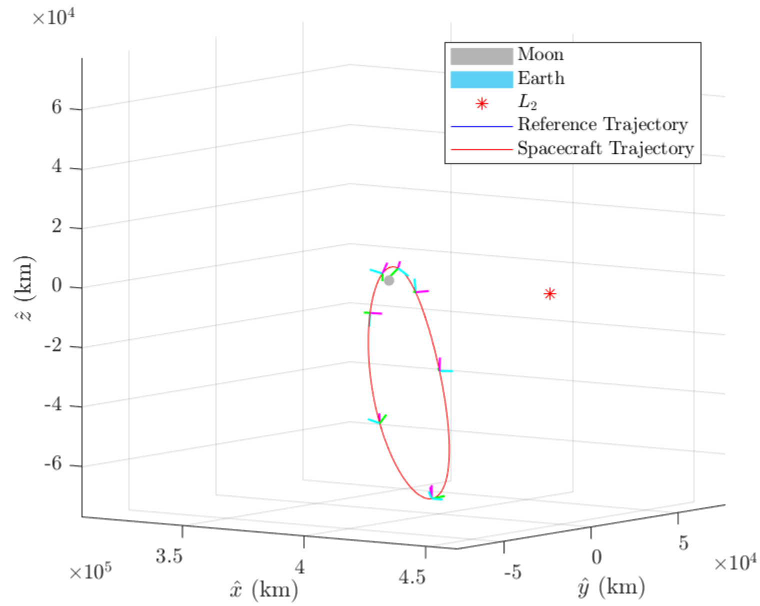

Fig. 4 Simulation with no Control Input

$$\mathfrak{se}(3) = \left\{ \boldsymbol{\Lambda} = \boldsymbol{\epsilon}^{\wedge} = \begin{bmatrix} \boldsymbol{e}^{\times} & \boldsymbol{\delta} \\ \boldsymbol{0}^T & 0 \end{bmatrix} \in \mathbb{R}^{4\times 4} \middle| \boldsymbol{\epsilon} = \begin{bmatrix} \boldsymbol{e} \\ \boldsymbol{\delta} \end{bmatrix} \in \mathbb{R}^6, \quad \boldsymbol{e}, \boldsymbol{\delta} \in \mathbb{R}^3 \right\} \tag{13}$$

Using Lie algebra, or geometric control, spacecraft 6DOF motions can be controlled, and the project proposes to develop convexified functions based on Lie Algebra for both governing cost function and path constraints. Using $SE(3)$ as the state variable form,

$$g = \begin{bmatrix} [SB] & \boldsymbol{R} \\ \boldsymbol{0}^T & 1 \end{bmatrix} \in \text{SE}(3) \tag{14}$$

where $R = \begin{bmatrix} x & y & z \end{bmatrix}^T$. Kinematics of this state variable is:

$$\begin{aligned} \dot{g} &= g\boldsymbol{v}^{\wedge} \\ &= g \begin{bmatrix} \boldsymbol{\omega}^{\times} & \boldsymbol{\nu} \\ \boldsymbol{0}^T & 0 \end{bmatrix} \end{aligned} \tag{15}$$

where $\boldsymbol{v} = \begin{bmatrix} \boldsymbol{\omega}^T & \boldsymbol{\nu}^T \end{bmatrix}^T$ is the combination of spacecraft translational and angular velocity. The rigid-body spacecraft dynamics eqautions governing translational and attitude motion are:

$$\begin{cases} \boldsymbol{J}\dot{\boldsymbol{\omega}} & = -(\omega)^{\times}\boldsymbol{J}\omega + \boldsymbol{M}_g([NB], \boldsymbol{R}) + \boldsymbol{\tau}' + \boldsymbol{\tau}'_d \\ m\dot{\boldsymbol{\nu}} & = m(\boldsymbol{\nu})^{\times}\omega + \boldsymbol{F}_g([NB], \boldsymbol{R}) + \boldsymbol{f}_{J_2}([NB], \boldsymbol{R}) + \boldsymbol{f}' + \boldsymbol{f}'_d \end{cases} \tag{16}$$

where m is the spacecraft mass, $\boldsymbol{J}$ is the spacecraft moment of inertia matrix in B-frame, $\boldsymbol{\tau}'$ and $\boldsymbol{f}'$ are the control input for rotational torque and translational force, $\boldsymbol{\tau}'_d$ and $\boldsymbol{f}'_d$ are the input perturbations, $\boldsymbol{M}_g$ and $\boldsymbol{F}_g$ are the gravity gradient moment and force, and $\boldsymbol{f}_{J_2}$ is the J_2 perturbing force caused by the bodies' oblateness. In this project, the gravity gradient moment and J_2 perturbing force caused by primary bodies' oblateness are neglected and substituted with Gaussian noise model. The accelerator control input can be expressed as $\boldsymbol{u} = \begin{bmatrix} \boldsymbol{\tau}^T & \boldsymbol{f}^T \end{bmatrix}^T = \mathcal{I}^{-1}\boldsymbol{u}' = \begin{bmatrix} \tau_1 & \tau_2 & \tau_3 & f_x & f_y & f_z \end{bmatrix}^T$, then Eq. 16 can be expressed in a compact form:

$$\mathcal{I}\dot{\boldsymbol{v}} = \mathrm{ad}_{\boldsymbol{v}}^{*}\mathcal{I}\boldsymbol{v} + \boldsymbol{\varphi} + \boldsymbol{u}' + \boldsymbol{u}'_d \tag{17}$$

where the spacecraft specification $\mathcal{I}$, gravitational force $\boldsymbol{\varphi}$, and the co-adjoint expression, $\mathrm{ad}_{\boldsymbol{\epsilon}}^{*}$, are

$$\mathcal{I} = \mathrm{diag}(\boldsymbol{J}, m\boldsymbol{I}_3) = \begin{bmatrix} I_1 & 0 & 0 & 0 & 0 & 0 \\ 0 & I_2 & 0 & 0 & 0 & 0 \\ 0 & 0 & I_3 & 0 & 0 & 0 \\ 0 & 0 & 0 & m & 0 & 0 \\ 0 & 0 & 0 & 0 & m & 0 \\ 0 & 0 & 0 & 0 & 0 & m \end{bmatrix} \tag{18}$$

$$\boldsymbol{\varphi} = \begin{bmatrix} \boldsymbol{0} \\ \boldsymbol{F}_g([NB], \boldsymbol{R}) \end{bmatrix} \tag{19}$$

$$\mathrm{ad}_{\boldsymbol{\epsilon}}^{*} = \begin{bmatrix} -\boldsymbol{e}^{\times} & -\boldsymbol{\delta}^{\times} \\ \boldsymbol{0}_{3\times3} & -\boldsymbol{e}^{\times} \end{bmatrix} \in \mathbb{R}^{6\times6} \tag{20}$$

Since $\mathrm{ad}_{\boldsymbol{\epsilon}}^{*}$ is an augmented combination of $\mathfrak{so}(3)$ which is already known to be an affine function, $\mathrm{ad}_{\boldsymbol{\epsilon}}^{*}$ is also an affine function. The non-convex part of this dynamics is the graviaty field model, $\boldsymbol{\varphi}$. To have this dynamics in the convex optimization problem, linearization is required as will be described in .

D. MPC Formulation

In this project, the model predictive control (MPC) method is used to control the spacecraft to achieve: 1) maintaining the desired orbit, 2) changing the attitude of the spacecraft to a desired attitude, and 3) satisfying 1) and 2) with minimum fuel usage. Construction of basic scenario describing the objective of the spacecraft in the mission is important in setting up a strategy for the control optimization and meeting the goals as designed. The situation was constructed as a model predictive control problem. In general, model predictive control calculates the optimal control for a system at the current time step, accounting for the future of the system through its dynamics. It also makes use of a moving horizon, where the optimal control is calculated at each time step using a consideration of the time evolution of the system forward in time only for a certain interval. Model predictive control is advantageous for station keeping around the L_2 point because the system is naturally unstable and susceptible to a variety of perturbations. Thus it is necessary to recalculate the optimal control as the spacecraft moves through its trajectory, not just at the beginning.

E. Convex Optimization Problem

Within the MPC algorithm, problem with convex functions is constructed. Throughout the MPC calculation process, the problem will be implemented within a closed loop and the convex problem will be solved using CVX. It is important to have the governing functions be convex, and since it is known that linear functions are convex, the equations of motions are linearized at g and v at the current MPC iteration. Since the dynamics are linear, the predicted g and v can be easily compared to the time-corresponding reference point. This eases the construction of the cost function. The SE(3) state variable has a property of having identity matrix for zero physical error, so $\boldsymbol{I}_4$ was subtracted from $\boldsymbol{h}$ and a Frobenius norm was taken for the magnitude of error where both position and attitude errors are concerned; the expression of this quantity is $||\boldsymbol{h} - \boldsymbol{I}_4||_F$, where the expression for $\boldsymbol{h}$ is shown in Eq. 21.

$$\boldsymbol{h} = (g^0)^{-1}g = \begin{bmatrix} [SB]_e & \boldsymbol{R}_e \\ \boldsymbol{0}^T & 1 \end{bmatrix} \quad \forall t \geq t_0 \tag{21}$$

In this case, as a Frobenius norm gives a scalar as a result, a weighing scalar instead of a usual weighing matrix Q is introduced. Since Frobenius norm is element-wise square sum and another weighing scalar is multiplied to it, the state cost function $J_g = \sum_k^N Q||\boldsymbol{h} - \boldsymbol{I}_4||_F$ is convex. Additionally, the control cost function may simply take the usual form of $J_{\boldsymbol{u}} = \sum_k^{N-1} \frac{1}{2}\boldsymbol{u}^T R\boldsymbol{u}$, which is indeed convex. For the input limit constraints, quadratic functions are introduced, formulating the final problem as:

$$
\begin{aligned}
\underset{x}{\text{minimize}} \quad & J_N = \sum_{k}^{N-1} Q||\boldsymbol{h}(k) - \boldsymbol{I}_4||_F + \frac{1}{2}\boldsymbol{u}(k)^T R\boldsymbol{u}(k) + Q||\boldsymbol{h}(N) - \boldsymbol{I}_4||_F \\
\text{subject to} \quad & \boldsymbol{\tau}^T\boldsymbol{\tau} \leq \tau_{max}^2 \\
& \boldsymbol{f}^T\boldsymbol{f} \leq f_{max}^2
\end{aligned}
\tag{22}
$$

and the strategy for solving the problem is described in Algorithm 1.

F. Results and Discussion

To implement the MPC algorithm, a southern halo orbit trajectory was first generated as mentioned previously. This initial trajectory will be used as the reference trajectory to control towards and to keep the spacecraft near the reference. After implementing Algorithm 1 in MATLAB with CVX, the output quantities were calculated, and the orthogonal view of the spacecraft performance and control input history over two reference orbital periods are shown in Fig. 5 and 6, respectively.

Fig.5 shows the reference trajectory in blue and the controlled trajectory in in red. The controlled trajectory shows both the resulting trajectory as well as the attitude of the of spacecraft. The results shown suggest that the optimized control using MPC and CVX does indeed work. The control scheme was able to generate a trajectory that is near the reference as well as adjusting the attitude in order to keep it oriented in the desired direction throughout its orbits. As mentioned in III.E, to analyze the performance of the controller, the error using the expression in terms of $\boldsymbol{h}$ at is calculated each time step, and its plot is shown in Fig. 7. A pure positional error plot in Cartesian coordinate system is shown in Fig. 8.

Even as there was arbitrary noise added to simulate environmental effects, the controller was able to keep course. The addition of perturbations would effect the trajectory at each iteration which, if uncorrected, would lead to accumulating error as mentioned previously where slight numerical changes would cause significant deviation down the line in Fig. 2. It is important to note that the result is not perfect and does not follow the reference trajectory perfectly. There are multiple ways to alleviate this error such as adjusting and tuning the weighting matrix Q which would result in more responsive control histories. Another way to reduce the error would be to increase the constraints to allow for stronger control influence, though these constraints may be set by requirements on certain physical systems.

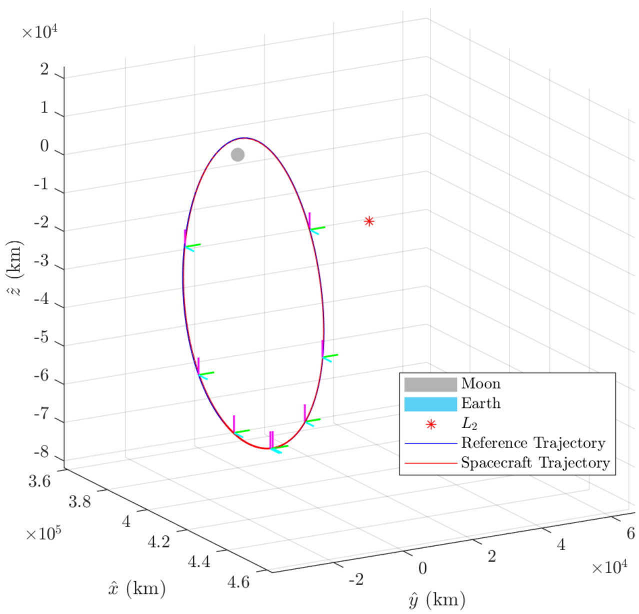

Fig. 5 Simulation with Optimal Control Input

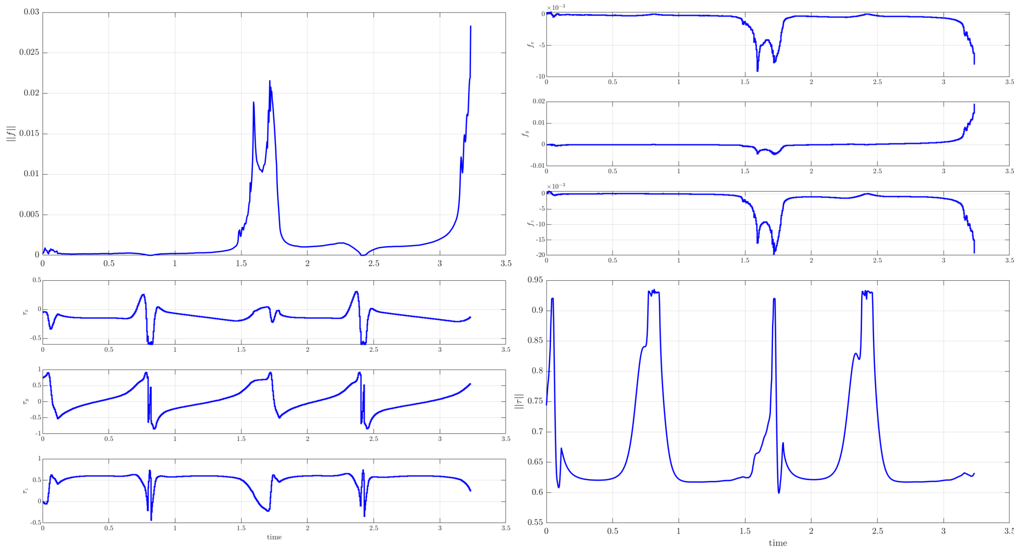

Fig. 6 Control Input History

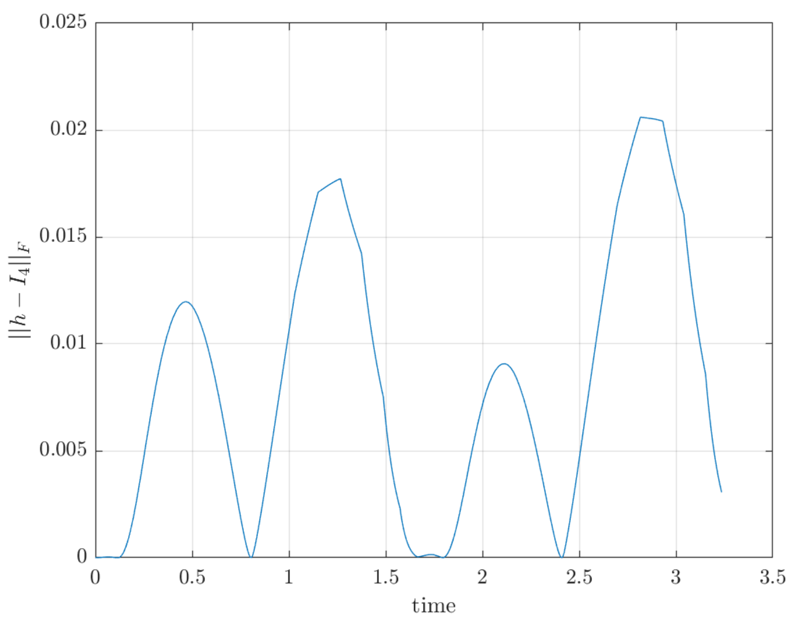

Fig. 7 6DOF Error History

G. Conclusion

The purpose of this project was to construct, apply, and analyze the use of convex optimization methods within the context of a non-linear control problem. It makes use of geometric control techniques, namely the construction of the dynamics using Lie groups and Lie algebras, to generate a control sequence that would achieve control of a 6DOF near a desired trajectory with certain constraints that would otherwise prove difficult to solve. In reality, many additional constraints, dynamics, and considerations must be taken in order to perfectly control such a system. Factors such as thruster specifications, environmental influences, and the speed of which the control scheme was generated. If given additional resources and time, these factors could be either incorporated within the model or within the control generation as well as be treated as external biases that the controller would have to overcome. These future topics would showcase and test the robustness of said controller against unknown circumstances if it were able to successfully do so.

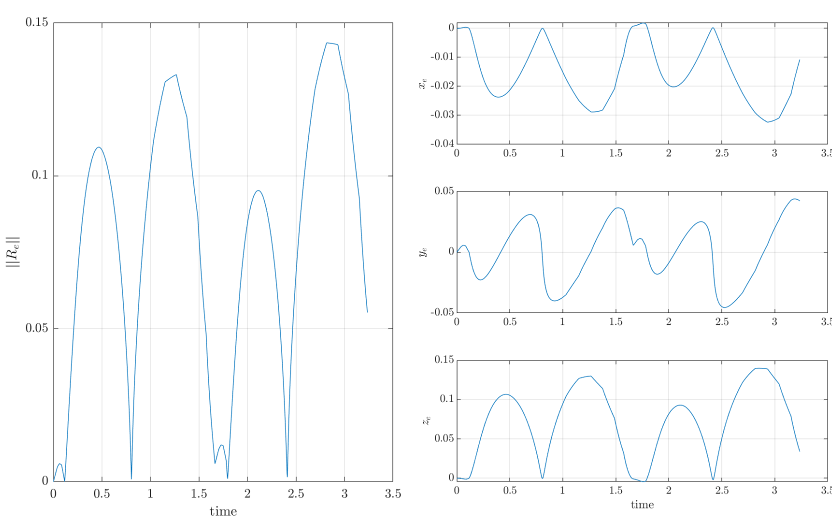

Fig. 8 Position Error History

Algorithm 1 MPC Implementation

Input: desired state history g_d
desired velocity history v_d
initial state $g(0) = g_0$
initial velocity $v(0) = v_0$
simulation time t_s
window time t_w
window size $N * 32$

Variables: time step $T = t_w / N$
MPC iteration $i_{MPC} = 0$
initial control guess $\boldsymbol{u}_g = \mathbf{0}$
window optimal control matrix $\boldsymbol{U}_N^*$
window optimal state matrix $\mathcal{G}_N^*$
window optimal velocity matrix V_N^*
complete optimal control matrix U^*
complete optimal state matrix $\mathcal{G}^*$
complete optimal velocity matrix V^*
perturbation vector $p \in \mathbb{R}^6$

while $i_{MPC} < t_s / T$ **do**
generate perturbations p
$v(0) \leftarrow v(0) + pT$
obtain state $g(i_{MPC})$ and $v(i_{MPC})$ ▹ using Eq. 3 6 and $u(i_{MPC} - 1)$
obtain state matrix A, B ▹ by performing linearization of Eq. 3 and 6 about $g(i_{MPC})$ and $v(i_{MPC})$
Solve: min $J_N(X, U)$ ▹ using interior-point method and CVX
subject to $g_1(\mathbf{W}) \leq 0$
given $g(0), g_d, v(0), v_d, \boldsymbol{u}_g$
set new $g(0)$ and $v(0)$ ▹ Using original nonlinear EoM
$U_g \leftarrow U_N^*$ ▹ set the next control guess to be the optimal control of the current iteration
$U^*(i_{MPC}) \leftarrow U_N^*(0)$ ▹ set the complete optimal control at the current step
$X^*(i_{MPC+1}) \leftarrow X_N^*(1)$ ▹ set the complete optimal state at the next step
$i_{MPC} \leftarrow i_{MPC} + 1$ ▹ increment the iteration counter
end while

Output: optimal control matrix U^*
optimal state matrix $\mathcal{G}^*$
optimal velocity matrix V^*

References

[1] Howell, K. C., “Three-Dimensional, Period, ’Halo’ Orbits,” *Celestial Mechanics*, Vol. 32, No. 1, 1984, pp. 53–71. https://doi.org/10.1007/BF01358403.

[2] Howell, K. C., and Pernicka, H. J., “Stationkeeping Method for Libration Point Trajectories,” *Journal of Guidance, Control, and Dynamics*, Vol. 16, No. 1, 1993, pp. 151–159. https://doi.org/10.2514/3.11440.

[3] Oguri, K., Oshima, K., Campagnola, S., Kakihara, K., Ozaki, N., Baresi, N., Kawakatsu, Y., and Funase, R., “EQUULEUS Trajectory Design,” *The Journal of the Astronautical Sciences*, Vol. 67, 2020, pp. 950–976. https://doi.org/10.1007/s40295-019-00206-y.